Nuclear-quadrupole-resonance study of pseudospin dynamics in a quasi-one-dimensional XY system

Sunyu Su and Robin L. Armstrong
Department of Physics, University of Toronto, Toronto, Ontario, Canada M5S 1A7

Wei Wei and Ron Donaberger
Neutron and Solid State Physics AECL Research, Chalk River, Ontario, Canada K0J 1J0

(Received 27 August 1990)

Nuclear-quadrupole-resonance (NQR) measurements of the spin-lattice relaxation rate (T_1^{-1}) for the halide nuclei in the praseodymium trihalides $PrCl_3$ and $PrBr_3$ are reported. They provide a significant test of the dynamical properties of the one-dimensional (1D) XY model as predicted within the Kubo linear-response regime. Measurements of ^{35}Cl T_1^{-1} values in $PrCl_3$ and ^{79}Br and ^{81}Br T_1^{-1} values in $PrBr_3$ have been made in the millikelvin temperature range where the 1D dynamical effects are enhanced. The data are shown to be in agreement with the predictions of a relaxation theory for a magnetic interaction, the theory is based on a rigorous treatment of the longitudinal dynamical correlation function $\langle S_z^m(t)S_z^n(0)\rangle$ of the electronic pseudospins S^m associated with the crystalline electric-field ground states. The fits to the data yield reasonable values for the hyperfine-interaction parameters A and the exchange integrals J/k_B.

I. INTRODUCTION

The XY model is of particular interest in the study of one-dimensional (1D) spin systems because it can be treated rigorously and because it represents a good starting approximation to other cases such as the isotropic Heisenberg model. Many of the properties of the model system have been calculated[1-6] and can, in principle, be compared with experiment. The difficulty is that very few physical realizations of the XY chain have been identified. The praseodymium trihalides, PrX_3, are among the best candidate crystals available.

The crystal structure of PrX_3 is shown in Fig. 1. The Pr ions form linear chains along the hexagonal crystal axes. Each X ion has three nearest-neighbor Pr ions. Electron-paramagnetic-resonance (EPR) measurements[7,8] of Pr pairs in $LaCl_3$ showed that the dominant Pr-Pr interaction is between nearest neighbors along the hexagonal axes. The symmetry at a Pr-ion site is C_{3h}. The crystalline electric-field splitting[9] of the $4f$ $^3H_4$ multiplet results in a non-Kramers ground-state doublet Γ_5.[10] As a result[11] the magnetic moment is parallel to the hexagonal axis and is rather small, giving a small $S_z^iS_z^{i+i}$ magnetic dipolar interaction. However, there is a strong coupling of the Pr doublets to E-symmetry transverse distortions, giving rise to a large XY interaction in an effective $S=\frac{1}{2}$ pseudospin representation which can be regarded as an antiferroelectric Jahn-Teller coupling.[12] The Hamiltonian describing the Pr-Pr interactions can therefore be written as

$$H_{i,i+1}=J_\perp(S_x^iS_x^{i+1}+S_y^iS_y^{i+1})+J_\parallel S_z^iS_z^{i+1}$$

with $J_\parallel/J_\perp \ll 1$. The Pr-Pr interaction in the praseodymium trihalides is therefore a good approximation to the XY model.

$PrCl_3$ has been the subject of numerous experimental investigations. Heat capacity and magnetic and electric susceptibility data[12-14] showed broad peaks near 1 K characteristic of 1D ordering and these features are well accounted for by the predictions of the XY model. A phase transition is observed at 0.4 K. Nuclear-quadrupole-resonance (NQR) results[15] provided conclusive evidence for a structural rather than a magnetic transition. The transition has been interpreted as a

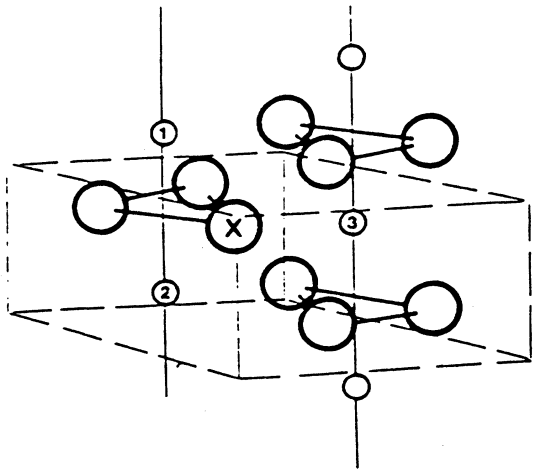

FIG. 1. Crystal structure of PrX_3. The small and large circles denote Pr ions and X ions, respectively. Pr ions 1, 2, and 3 are nearest neighbors to the labeled X ion. The dashed lines indicate a unit cell.

cooperative Jahn-Teller transition to a 3D antiferroelectric ordered state[12] which has been predicted to be a Peierls dimerization.[16]

Electric susceptibility measurements[17] on $PrBr_3$ suggest that its low-temperature behavior is also that of a 1D XY chain.

A few experimental investigations of the dynamical properties of the XY chains in $PrCl_3$ have been reported and found to be in agreement with the theoretical predictions. Infrared absorption measurements[18] yielded a peak due to absorption by $\mathbf{k}=\mathbf{0}$ spin excitations, and electronic Raman scattering line shapes[19] were measured and found to be in agreement with the theory.

NQR is an important technique for the study of spin dynamics in these 1D systems. The dynamical longitudinal properties of the 1D XY model have been obtained by Katsura, Horiguchi, and Suzuki[5] using the two-time Green-function method within the Kubo linear-response regime. An equivalent treatment has been given by Niemeijer.[3] The fact that the longitudinal dynamical correlation function $\langle S_z^m(t)S_z^n(0)\rangle$ is rigorously known at all temperatures permits a theoretical prediction of the X nuclear spin relaxation rate (T_1^{-1}) as a function of temperature. The first T_1^{-1} data reported[20] were for the ^{35}Cl nuclei in $PrCl_3$. They were analyzed in terms of a nuclear relaxation theory developed by Moriya.[21] The analysis yielded a value for the exchange integral J/k_B ($J\equiv J_\perp$) of less than 0.9 K, inconsistent with the values obtained from specific-heat and susceptibility measurements. These data were subsequently reanalyzed[22] using the equations of Katsura, Horiguchi, and Suzuki.[5] The results were inconclusive due to the large scatter associated with the experimental data, but it seemed unlikely that they could be explained using a reasonable value for the parameter J.

In Sec. II we present new ^{35}Cl NQR T_1^{-1} data for $PrCl_3$ taken in the 1D regime; we also present ^{79}Br and ^{81}Br T_1^{-1} data for $PrBr_3$. Each data set is compared with theoretical calculations in Sec. III. The paper concludes with a brief summary in Sec. IV.

II. EXPERIMENTAL

The samples of $PrCl_3$ and $PrBr_3$, consisting of an assortment of small single crystals, were obtained from D. R. Taylor, Queen's University, Kingston, Ontario. They were identified by their characteristic halide NQR frequencies. The samples were placed in Pyrex cylinders and stored in an inert atmosphere. Liquid helium was introduced into the sample tubes before the experiments and maintained in the tubes during the experiments to ensure good thermal contact between the single crystals and their surroundings.

An Oxford Instrument 200-μW dilution refrigerator was used to obtain the millikelvin temperatures required for the experiments. The coaxial cable used as the rf transmission line between the sample coil and the tuning circuit on top of the cryostat was a cyrogenic 50-Ω semirigid (model UT T-85-SS-SS) cable manufactured by Micro Coax Components, Inc. Both inner and outer conductors were of stainless steel. Care was taken to thermally anchor the coaxial cable to the 4.2-K pot in the dilution refrigerator.

The NQR T_1^{-1} measurements were taken using a conventional NMR pulsed spectrometer. The NQR frequencies at 4.2 K were 4.5667 MHz for the ^{35}Cl resonance, 30.747 MHz for the ^{81}Br resonance, and 36.802 MHz for the ^{79}Br resonance. The resonance frequencies were essentially temperature independent over the temperature range of the experiments. The pulse sequences were generated by a PULS-kit unit and signal averaging was performed by a SA-kit unit; both units were manufactured by Tecmag, Inc. A Tecmag software package named MACNMR was used to control the NQR experiments. The actual rf pulses were created by gating the output of a Fluke 616B synthesizer, which was then amplified by an Amplifier Research 200L power amplifier. The NQR signals from the sample coil were amplified by a two-stage 5–500 MHz Avantek UTO-517 broadband amplifier. The amplified signals were detected in phase quadrature, digitized and averaged, and subsequently analyzed using a Macintosh II computer.

The pulse sequence used to measure the T_1^{-1} values was a $\pi/2$-τ-$\pi/2$ sequence. Since rf heating of the sam-

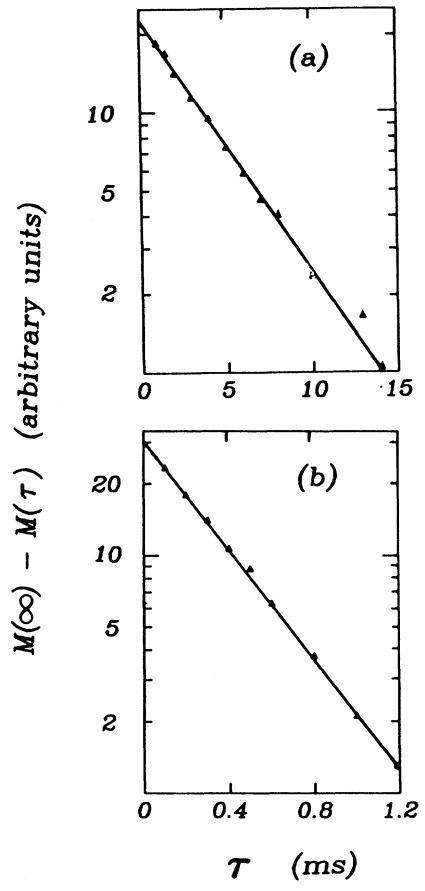

FIG. 2. Magnetization recovery curves for (a) the ^{35}Cl resonance in $PrCl_3$ at 2.4 K and (b) the ^{81}Br resonance in $PrBr_3$ at 2.4 K.

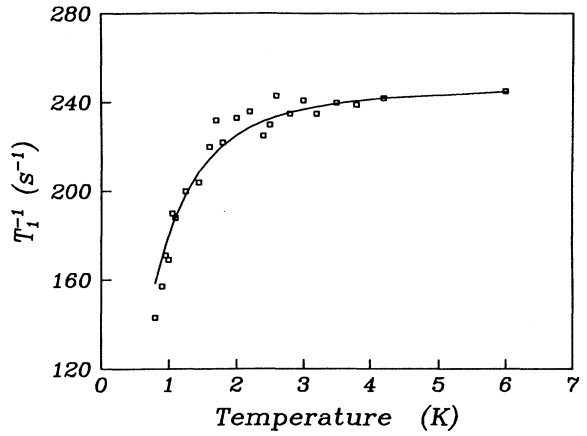

FIG. 3. The temperature dependence of T_1^{-1} for ^{35}Cl in $PrCl_3$. The symbols □ are experimental data. The solid line is the theoretical prediction for $J/k_B = 2.2$ K.

ple was an important consideration, this pulse sequence, with an appropriate repetition rate, was chosen to minimize the heat input. A typical $\pi/2$ pulse length for $PrCl_3$ was 17 μs, and for $PrBr_3$ was 5.5 μs.

Typical magnetization recovery curves are shown in Fig. 2; (a) shows the ^{35}Cl magnetization recovery in $PrCl_3$ at 2.4 K, and (b) the ^{81}Br magnetization recovery in $PrBr_3$. In each case the recovery is exponential as expected for a spin-$\frac{3}{2}$ NQR system. Note that the recovery of the ^{81}Br magnetization is an order of magnitude faster than the recovery of the ^{35}Cl magnetization. This result reflects the much larger quadrupole coupling constant for ^{81}Br as compared to ^{35}Cl. Note that the ^{81}Br data show less scatter than the ^{35}Cl data because of the better signal-to-noise ratio at the higher ^{81}Br frequency. The spin-lattice-relaxation time (T_1) is obtained directly from the slope of the straight lines in this type of semilogarithmic plot; T_1^{-1} is the reciprocal of T_1. The statistical error associated with the determination of the T_1^{-1} values

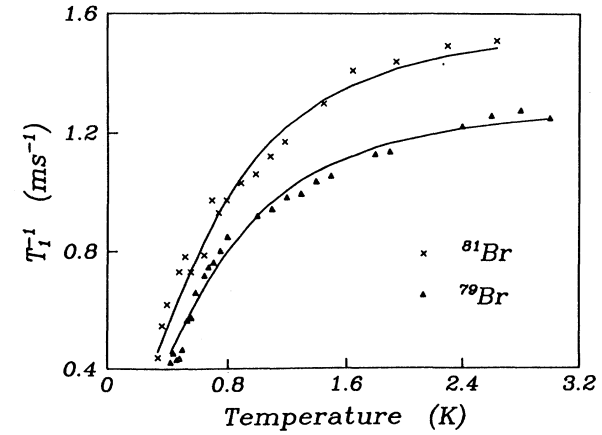

FIG. 4. The temperature dependence of T_1^{-1} for ^{79}Br and ^{81}Br in $PrBr_3$. The symbols △, × are experimental data. The solid lines are the theoretical predictions for $J/k_B = 2.35$ K.

is about 5% for $PrCl_3$ and 3% for $PrBr_3$.

The temperature dependence of T_1^{-1} for the ^{35}Cl resonance in $PrCl_3$ is shown in Fig. 3. The results are consistent with those previously reported[20] but the scatter is significantly less. For the earlier data the statistical scatter is $> 10\%$.

The temperature dependencies of T_1^{-1} for the ^{79}Br and ^{81}Br resonances in $PrBr_3$ are shown in Fig. 4. We note the following: (a) The results are qualitatively similar to those of Fig. 3; (b) the ^{81}Br data lie above the ^{79}Br data. The second observation is a dramatic illustration that the nuclear spin-lattice relaxation is dominated by the magnetic dipole interaction and not by the electric quadrupole interaction. If the latter were true, the ^{81}Br data would lie below the ^{79}Br data.

III. ANALYSIS AND DISCUSSION

A general expression for T_1^{-1} due to fluctuating magnetic fields $H_q(t)$ at the site of the resonant nucleus is given by[23]

$$T_1^{-1} = \gamma_n^2 [k_{xx}(\omega_0) - k_{yy}(\omega_0)] ,$$

where

$$k_{qq'}(\omega) = \tfrac{1}{2} \int_{-\infty}^{+\infty} \langle H_q(t) H_{q'}(0) \rangle e^{i\omega t} dt ,$$

where γ_n is the nuclear gyromagnetic ratio. In the present case the fluctuating magnetic fields at the X nuclear sites are assumed to arise solely from the magnetic moments of the nearest-neighbor Pr ions. This is a good approximation since magnetic contributions to T_1^{-1} fall off at least as rapidly as r^{-6}. The Pr ions labeled 1 and 2 in Fig. 1 are 3.0 Å from the X site and make angles of $\pm 45°$ with the mirror symmetry plane through the X sites. Their magnetic moments (proportional to S_z^m) generate magnetic fields at X site with components parallel and perpendicular to the hexagonal axis; the perpendicular component contributes to T_1^{-1}. The Pr ion labeled 3 generates neither an H_x nor an H_y component at the X site and hence gives no contribution to T_1^{-1}. The hyperfine interaction between the Pr ion labeled m and the X nucleus is of the form $[A' S_z^m I_z + A(S_z^m I_x + S_z^m I_y)]$, where I refers to the nuclear angular momentum and $A'A$ are Pr-X hyperfine-interaction constants. The contribution of Pr ions 1 and 2 to the X nuclear T_1^{-1} is then readily shown to be[24]

$$T_1^{-1} = A^2 [\Phi_{zz}^{11}(\omega) - \Phi_{zz}^{12}(\omega)] ,$$

where ω is the NQR resonance frequency. The quantity $\Phi_{zz}^{mn}(\omega)$ is given by

$$\Phi_{zz}^{mn}(\omega) = \int_{-\infty}^{+\infty} \Phi_{zz}^{mn}(t) e^{i\omega t} dt ,$$

where $\Phi_{zz}^{mn}(t)$ is the time-dependent, longitudinal correlation function of spin m and spin n

$$\Phi_{zz}^{mn}(t) = \langle S_z^m(t) S_z^n(0) \rangle .$$

A general expression for $\Phi_{zz}^{mn}(t)$ has been given as[5]

$$\Phi_{zz}^{mn}(t)=(4\pi)^{-2}\int_0^{2\pi}dq\int_0^{2\pi}dp\,\exp[i(m-n)(p-q)]\exp[iJt(\cos p-\cos q)/\hbar]$$
$$\times[1+\tanh(\beta/2\cos p)][1-\tanh(\beta/2\cos q)]\ ,$$

where $\beta=(J/k_BT)$ and J in the above expressions are twice those of Ref. 5. The Fourier transforms of the autocorrelation and pair-correlation functions have been shown to be given by

$$\Phi_{zz}^{11}(\tilde{\omega})=\left[\frac{\hbar}{\pi J}\right]\int_0^{1-(1/2)\tilde{\omega}}dx\frac{[1+\tanh(\frac{1}{4}\beta\tilde{\omega})]^2[1+\mathrm{sech}^2(\frac{1}{4}\beta\tilde{\omega})\sinh^2(\frac{1}{2}\beta x)]^{-1}}{[(1+\frac{1}{2}\tilde{\omega})^2-x^2]^{1/2}[(1-\frac{1}{2}\tilde{\omega})^2-x^2]^{1/2}}\ ,$$

$$\Phi_{zz}^{12}(\tilde{\omega})=\left[\frac{\hbar}{\pi J}\right]\int_0^{1-(1/2)\tilde{\omega}}dx\frac{[1+\tanh(\frac{1}{4}\beta\tilde{\omega})]^2[1+\mathrm{sech}^2(\frac{1}{4}\beta\tilde{\omega})\sinh^2(\frac{1}{2}\beta x)]^{-1}}{[(1+\frac{1}{2}\tilde{\omega})^2-x^2]^{1/2}[(1-\frac{1}{2}\tilde{\omega})^2-x^2]^{1/2}}(x^2-\tfrac{1}{4}\tilde{\omega}^2)\ ,$$

where $\tilde{\omega}=\hbar\omega/J$.

The expression for T_1^{-1} can then be written as

$$T_1^{-1}=\left[\frac{A^2}{\pi J}\right]\int_0^{1-(1/2)\tilde{\omega}}dx\frac{[1+\tanh(\frac{1}{4}\beta\tilde{\omega})]^2[1+\mathrm{sech}^2(\frac{1}{4}\beta\tilde{\omega})\sinh^2(\frac{1}{2}\beta x)]^{-1}}{[(1+\frac{1}{2}\tilde{\omega})^2-x^2]^{1/2}[(1-\frac{1}{2}\tilde{\omega})^2-x^2]^{1/2}}(1-x^2+\tfrac{1}{4}\tilde{\omega}^2)\ .$$

An analytic expression for T_1^{-1} is, in general, unobtainable. Neither the high-temperature nor the low-temperature approximation, for which analytic expressions can be derived, is appropriate since the temperature range of interest is comparable to J/k_B. Therefore, theoretical predictions of the temperature dependence of T_1^{-1} must be made by numerical integration of the full expression for a series of temperatures. The parameter A is first obtained by choosing a value of J/k_B and fitting to the high-temperature data. With this value for A, theoretical predictions for T_1^{-1} values over the entire temperature range are then made. The process is repeated for a series of values of J/k_B and the resultant curves compared to the experimental data to obtain a best fit.

The solid curve in Fig. 3 represents a best fit to the ^{35}Cl data for $PrCl_3$. The parameters which describe the curve are $A=(4.70\pm0.03)\ s^{-1}$ and $J/k_B=(2.2\pm0.2)$ K. The important point is that the pair-correlation contribution is of comparable importance to the autocorrelation contribution. It is not possible to adequately represent the data with only an autocorrelation contribution. The value of A may be compared with the estimated magnetic dipolar interaction between a Cl nucleus and a Pr neighbor, namely, $g_\parallel g_N\mu_B\mu_N/\hbar r^3\simeq1.5\times10^6\ s^{-1}$. In view of the simplistic nature of this estimate, we conclude that our value for A is quite reasonable. The value of J/k_B compares well with the most recent published value,[19] namely, 2.4 ± 0.2 K.

In the earlier reanalysis[22] of the Mangum and Thornton data[20] only the autocorrelation contribution was considered. Further, the theoretical curve was deduced by using a high-temperature expansion for T_1^{-1} rather than by numerical integration of the full expression.

The solid curves in Fig. 4 represent the best fits to the ^{79}Br and ^{81}Br data for $PrBr_3$. In each case the value of the parameter J/k_B is 2.35 K. The hyperfine parameters are $A(^{79}Br)=(1.12\pm.02)\times10^6\ s^{-1}$ and $A(^{81}Br)=(1.24\pm0.02)\times10^6\ s^{-1}$. The ratio $[A(^{81}Br)/A(^{79}Br)]^2=1.11\pm0.07$ is in good agreement with the ratio of nuclear magnetic moments $[\mu(^{81}Br)/\mu(^{79}Br)]^2=1.16$.

The only previously reported value of J/k_B for $PrBr_3$, from the analysis of electric susceptibility data, is 3.0 K. It is interesting to note that the difference in J/k_B values for $PrCl_3$ and $PrBr_3$ as deduced from susceptibility experiments is 0.15 K with J/k_B for $PrBr_3$ greater than J/k_B for $PrCl_3$. This is precisely the same difference that we have deduced from the NQR measurements of T_1^{-1}.

IV. CONCLUSIONS

This experiment has provided a direct and rigorous test of certain dynamical properties of the 1D XY model. The measurements on the two isotopes of bromine give irrefutable evidence of the dominance of the magnetic dipole interaction as the mechanism for nuclear spin-lattice relaxation in $PrBr_3$. The importance of the electronic-spin pair-correlation-function contribution to T_1^{-1}, in addition to the autocorrelation-function contribution, is illustrated. The analysis of the NQR data gives quantitative values for the exchange integrals which are consistent with those obtained from other experiments, and reasonable values for the hyperfine-interaction parameters.

ACKNOWLEDGMENTS

We wish to express our thanks to D. R. Taylor for providing the samples and for several discussions and to H. F. Nieman for technical assistance. We also wish to thank J. S. Waugh for sharing his experience with NMR experiments in the millikelvin range.

[1]E. Lieb, T. Schultz, and D. Mattis, Ann. Phys. (N.Y.) **16**, 407 (1961).
[2]S. Katsura, Phys. Rev. B **127**, 1508 (1962).
[3]Th. Niemeijer, Physica (Utrecht) **36**, 377 (1967).
[4]Th. Niemeijer, Physica (Utrecht) **39**, 313 (1968).
[5]S. Katsura, T. Horiguchi, and M. Suzuki, Physica (Utrecht) **46**, 67 (1970).
[6]J. H. H. Perk and H. W. Capel, Physica (Utrecht) **89A**, 265 (1977).
[7]J. W. Culvahouse, D. P. Schinke, and L. G. Pfortmiller, Phys. Rev. **177**, 454 (1969).
[8]J. W. Culvahouse and L. Pfortmiller, Bull. Am. Phys. Soc. **15**, 394 (1970).
[9]B. R. Judd, Proc. R. Soc. London, Ser. A **241**, 414 (1957).
[10]G. H. Dieke, *Spectra and Energy Levels of Rare Earth Ions in Crystals* (Interscience, New York, 1968).
[11]A. Abragam and B. Bleaney, *Electron Paramagnetic Resonance of Transitions Ions* (Clarendon, Oxford, 1970).
[12]J. P. Harrison, J. P. Hessler, and D. R. Taylor, Phys. Rev. B **14**, 2979 (1976).
[13]J. H. Colwell, B. W. Mangum, and D. B. Utton, Phys. Rev. **181**, 842 (1969).
[14]T. Folinsbee, J. P. Harrison, D. B. McColl, and D. R. Taylor, Phys. Rev. B **14**, 2979 (1976).
[15]J. P. Hessler and E. H. Carlson, J. Appl. Phys. **42**, 1316 (1971).
[16]R. M. Morra, R. L. Armstrong, and D. R. Taylor, Phys. Rev. Lett. **51**, 809 (1983).
[17]D. R. Taylor, J. P. Harrison, and D. B. McColl, Physica **86-88B**, 1164 (1977).
[18]M. Beirs, A. J. Sievers, J. P. Harrison, D. R. Taylor, and D. J. Thouless, Phys. Rev. Lett. **41**, 987 (1978).
[19]E. Goovaerts, D. De Readt, and D. Schoemaker, Phys. Rev. Lett. **52**, 1649 (1984).
[20]B. W. Mangum and D. D. Thornton, Phys. Rev. Lett. **22**, 1105 (1969).
[21]T. Moriya, Prog. Theor. Phys. (Kyoto) **16**, 23 (1956).
[22]M. D'Iorio, R. L. Armstrong, and D. R. Taylor, Phys. Rev. B **27**, 1664 (1983).
[23]C. P. Slichter, *Principles of Magnetic Resonance* (Springer-Verlag, New York, 1990), Chap. 5.
[24]M. Myers and A. Narath, Phys. Rev. Lett. **27**, 641 (1971).